Biologically-Induced Transport Modeling for the Clive DU PA

28 May 2011

Prepared by

Neptune and Company, Inc.

This page is intentionally blank, aside from this statement.

CONTENTS

FIGURES

TABLES

1.0 Summary of Parameters

Following is a brief summary of input values used parameters employed in the biotic transport component of the Clive Performance Assessment (PA) model that is the subject of this white paper.

Table 1 lists the biological transport model parameter distributions for the Clive DU waste cell GoldSim Model that are summarized in this document. For a number of biotic parameters, site specific data were not available for the Clive site, so the GoldSim model makes use of biotic parameters for the same or similar species developed for the performance assessment of disposal cells at the Nevada National Security Site (NNSS, formerly the Nevada Test Site), with the assumption that these species-specific parameters do not vary greatly across North American desert types. The derivation of these NNSS parameters is detailed in the relevant NNSS documents (Neptune 2005a, 2005b, 2006).

For distributions, the following notation is used:

- N(μ, σ, [*min*, *max*]) represents a normal distribution with mean μ and standard deviation σ, and optional truncation at the specified *min*imum and *max*imum,
- LN(*GM*, *GSD*, [*min*, *max*]) represents a log-normal distribution with geometric mean *GM* and geometric standard deviation *GSD*, and optional *min* and *max*,
- U(*min*, *max*) represents a uniform distribution with lower bound *min* and upper bound *max*,
- Beta(μ, σ, *min*, *max*) represents a generalized beta distribution with mean μ, standard deviation σ, minimum *min*, and maximum *max*,
- Gamma(μ, σ) represents a gamma distribution with mean μ and standard deviation σ, and
- TRI(*min*, *m*, *max*) represents a triangular distribution with lower bound *min*, mode *m*, and upper bound *max*.

Table 1. Summary of Biotic Transport Parameters

Parameter	Value	Units	Reference / Comment
Ant Transport Parameters			
Volume of Each Nest	N(μ=0.161, σ=0.024, min=0, max=Large)	m^3	SWCA, 2011 (Sec 2.3, Appendix A1) and Neptune, 2006. See Section 4.3
Lifespan of Each Colony	N(μ=20.2, σ=3.6, min=0, max=Large)	yr	Neptune, 2006 (Section 6.8, p. 16)
ColonyDensity - area density of colonies on the ground	___	___	SWCA, 2011 (Table 20, p. 23). See Section 4.7
ColonyDensity_Plot1	Gamma(33,1, min=0, max=Large)	1/ha	*Ibid.*
ColonyDensity_Plot2	Gamma(2, 1, min=0, max=Large)	1/ha	*Ibid.*
ColonyDensity_Plot3	Gamma(7, 1, min=0, max=Large)	1/ha	*Ibid.*
ColonyDensity_Plot4	Gamma(17, 1, min=0, max=Large)	1/ha	SWCA, 2011 (Based on provided data. Information for this plot in Table 20, p. 23 in the SWCA report is incorrect.)
ColonyDensity_Plot5	Gamma(6, 1, min=0, max=Large)	1/ha	*Ibid*
MaxDepth - maximum depth for any colony	212	cm	SWCA, 2011 and Neptune, 2006. See Section 4.4.
b - fitting parameter for nest shape	N(μ=10, σ=0.71, min=1, max=Large)	—	Neptune, 2006 (Section 7.3, p. 21)

Mammal Transport Parameters			
MoundDensity - area density of mounds on the ground	see below for each plot	---	SWCA, 2011 (Section 2.2.2, p. 18 – 22)
_Plot1	Gamma(235, 1, min=0, max=Large)	1/ha	
_Plot2	Gamma(239, 1, min=0, max=Large)	1/ha	
_Plot3	Gamma(1.33, 1, min=0, max=Large)	1/ha	
_Plot4	Gamma(1.33, 1, min=0, max=Large)	1/ha	
_Plot5	Gamma (1.33, 1, min=0, max=Large)	1/ha	
ExcavationRate - volumetric rate of a single burrow excavation	N(μ=0.0006, σ=0.00015, min=Small, max=Large)	m^3/yr	Mean of excavated volumes at each sample location from SWCA, 2011 (Tables 13, 15, 17, 19), corrected for the number of burrows reported at each sample location (See Table 14 of this white paper)
MaxDepth - maximum depth for any burrow	200	cm	Neptune 2005b (Table 2)
b - fitting parameter for burrow shape	N(μ=4.5, σ=0.84, min=1, max=Large)	—	Fitting parameter for rodent burrows from Neptune 2005b (Fig. 10, p. 22)
Plant Transport Parameters			
BiomassProductionRate	U(300,1500)	kg/ha yr	Approximate Range for Great Basin from Smith, et al 1997(Fig 7, p. 37)
PctCover_Plot*_[plant]	Tabulated in Clive PA Model Parameters.xls workbook	—	Simulations based on SWCA (2011) percent cover data. See Section 3.3

Percent cover random selector	randomly select between values 1 to 1000, inclusive	—	Modeling construct
Vegetation Association Picker	Discrete (1, 2, 3, 4, 5)	—	Modeling construct
Greasewood Parameters			
RootShoot_Ratio	U(0.30, 1.24)	—	Assumed similar to creosote, Neptune, 2005a (Table 16, p. 38)
MaxDepth	570	cm	Robertson, 1983 (p. 311)
b - fitting parameter for root shape	N(μ=14.6, σ=0.0807, min=1, max=Large)	—	Assumed similar to creosote, Neptune, 2005a (Fig. 9, p. 51)
RootShoot_Ratio	T(1, 1.2, 2)	—	Mode based on Bethlenfalvay and Dakessian, 1984 (Table 2, p. 314); bounds based on Neptune, 2005a
MaxDepth	150	cm	Based on H. comata from Zlatnik, 1999a (p. 7)
b - fitting parameter for root shape	N(μ=2.19 σ=0.036, min=1, max=Large)	—	For perennial grasses, from Neptune 2005a (Fig. 12, p. 55)
Forb Parameters			
RootShoot_Ratio	U(0.40, 1.80)	—	Distribution of “Other Shrubs” used for conservatism, see Section 3.4
MaxDepth	51	cm	Based on Halogeton, from Pavek, 1992 (p. 5)
b – fitting parameter for root shape	N(μ=23.9 σ =0.313, min=1, max=Large)	—	Distribution same as “Other Shrubs”, see Section 3.5
Tree Parameters			
RootShoot_Ratio	U(0.55, 0.76)	—	For Juniperus occidentalis from Miller et al., 2005 (p. 16)

MaxDepth	450	cm	For J. occidentalis from Zlatnik, 1999b (p. 6)
b – fitting parameter for root shape	N(μ=14.6 σ=0.0807, min=1, max=Large)	—	Distribution for creosote used due to similar taproot depth, see Section 3.5
Other Shrub Parameters			
RootShoot_Ratio	U(0.4, 1.8)	—	Based on range for Artemisia sp. from Neptune, 2005a (Table 16, p. 38),
MaxDepth	110	cm	Branson et al. 1976 (Fig. 19, p. 1120)
b - fitting parameter for nest shape	N (μ= 23.9, σ=0.313, min=1, max=Large)	—	Based on fitting parameter for Atriplex canascens at NNSS, from Neptune 2005a (Fig 10, p. 52)
Plant/Soil Concentration Ratios			
PlantCRs by chemical element	tabulated in Clive PA Model Parameters.xls workbook	—	See Table 10
Plant CR GM for Rn	Small	—	See Table 10
Plant CR GSD for Rn	1	—	See Table 10

2.0 Introduction

Biotic fate and transport models have been developed for the depleted uranium (DU) waste cell at the Clive repository to evaluate the redistribution of soils, and contaminants within the soil, by native flora and fauna. The biotic models are part of a larger Performance Assessment (PA) model that has been built to evaluate the consequences of contaminant migration over time from the DU waste cell. The purpose of the PA model is to provide a decision management system that will support future disposal, closure and long term monitoring decisions, as well as supporting all regulatory requirements of PAs and other environmental assessments for these waste disposal systems. The Clive facility is located in the eastern side of the Great Salt Lake Desert, with flora and fauna characteristic of Great Basin alkali flat and Great Basin desert shrub communities.

3.0 Plant Specifications and Parameters

The purpose of this chapter is to explain the component of the Clive PA model that addresses calculation of plant-mediated contaminant mass distributions by depth, and the rate of contaminant transport from subsurface strata to the ground surface.

3.1 Plant Conceptual Model

Plant-induced transport of contaminants is assumed to proceed by absorption of contaminants into the plants roots, followed by redistribution throughout all the tissues of the plant, both above ground and below ground. Upon senescence, the above-ground plant parts are incorporated into surface soils, and the roots are incorporated into soils at their respective depths (Figure 1).

The calculations of contaminant transport due to plant uptake and redistribution take place in a series of steps:

1. Calculate the fraction of plant roots in each layer for each plant type.

2. Calculate uptake of contaminants into plant roots in each layer.

3. Sum the contaminant uptake to determine the total uptake by the roots for each contaminant.

4. Determine the average concentration in the roots, assuming complete redistribution within the root mass.

5. Assuming that the plant returns all fixed contaminants to adjacent soils upon senescence, determine how much of each contaminant is returned to each layer. The aboveground plant parts are mixed in the uppermost layer.

6. Calculate uptake of contaminants into aboveground parts of the plant ("shoots"), based on the fractions of roots fixing contaminants within each layer and sending it up to the shoots.

7. Calculate the net flux of contaminants into (or out of) each layer due to steps 1 through 6. This value is used to adjust contaminant inventories in each layer (each layer is a GoldSim cell).

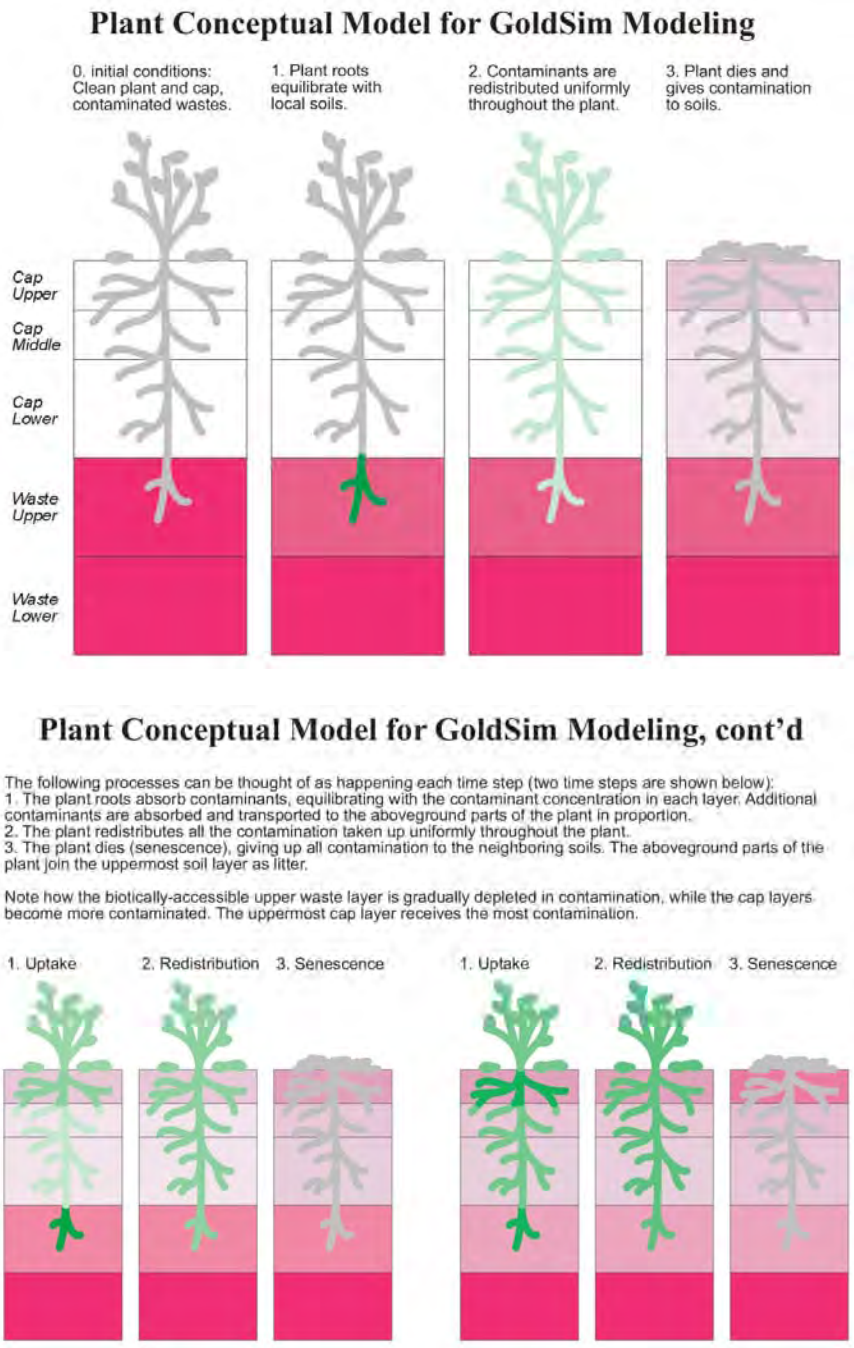

Figure 1. Conceptual model of contaminant uptake and redistribution by plants

This section describes the functional factors that contribute to the parameterization of the plant section of the biotic transport model. Such factors include identifying dominant plant species, grouping plant species into categories that are significantly similar in form and function with respect to the transport processes, estimating net annual primary productivity (NAPP, a measure of combined above-ground and below-ground biomass generation), determining relative abundance of plants or plant groups, evaluating root/shoot mass ratios, and representing the density of plant roots as a function of depth below the ground surface. The data used for each of the seven steps of the algorithm are presented, outstanding issues with the available data are identified, and the issues that deserve attention for the next model iteration are described.

In the Clive DU PA model, the vertical soil horizon is discretized into horizontal layers based on various functional attributes of the soil-based biotic communities (plants and animals), requirements related to gas and liquid transport, and the configuration of the disposal cell cover. The model is ultimately used to simulate radionuclide transport throughout the soil layers. Utilizing the information provided in 1 through 6 above, distributions of above-ground and below-ground NAPP for grasses, forbs, shrubs and trees are developed. Radionuclide activity associated with above-ground biomass is assigned to the uppermost soil/cover layer in the model. Radionuclide activity associated with below-ground NAPP is apportioned by depth interval according to root mass distribution. In order to reflect the redistribution of radionuclides, these calculations require the use of plant uptake factors (plant-soil concentration ratios) to model the relative uptake of contaminants from soil by plants.

3.2 Identification of Plant Functional Groups

Field surveys of the Clive site and surrounding areas were conducted by SWCA Environmental Consultants in September and December 2010 to identify plant species present in different vegetative associations around the Clive Site (SWCA Environmental Consultants, 2011). Five different vegetative associations were surveyed, with three associations representing the alkali flat/desert flat type soils found in the vicinity of Clive, and two associations representative of desert scrub/shrub-steppe habitat characteristic of slopes and slightly higher elevations with less-saline soil chemistry. A one hectare (100 m × 100 m) plot was established in each vegetative association, and each plot was surveyed for dominant plant species present, and the percent cover and density of each species. In addition, a small number of black greasewood, shadscale, halogeton, and Mojave seablite plants were excavated to obtain root profile measurements and above-ground plant dimensions. The vegetative associations for each plot are shown in Table 2. Plots 3 through 5 represent current vegetation at the Clive site, while Plots 1 and 2 are representative of less-saline soils that may develop on top of the waste cell cover.

A total of 41 plant species were identified on the five survey plots. Eighteen species each comprised at least 1% of the total cover on at least one plot. These 18 species were considered the most important for purposes of modeling plant mediated transport of chemical contaminants at Clive. Species were grouped into five functional plant groups, as shown in Table 3. The five functional groups are: grasses, forbs, greasewood, other shrubs, and trees. Greasewood is separated from other shrubs due to its status as a phreatophyte that can extend taproots in excess of five meters to reach groundwater. Annual and perennial grasses were grouped due to similar maximum rooting depths.

Table 2. Vegetative associations surveyed for embankment cover modeling

Plot Number	Plot Name
1	Mixed Grassland
2	Juniper-sagebrush
3	Black Greasewood
4	Halogeton-disturbed
5	Shadescale-Gray Molly

Table 3. Species identified at Clive included within each plant group

Plant Group	Common Name	Species Name
Forbs	Halogeton	*Halogeton glomeratus*
Forbs	Mojave seablite	*Suaeda torreyana*
Forbs	Curveseed butterwort	*Ranunculus testiculatus*
Grasses	Needle and thread	*Hesperostipa comata*
Grasses	Intermediate wheatgrass	*Thinopyrum intermedium*
Grasses	Sandberg bluegrass	*Poa secunda*
Grasses	Crested wheatgrass	*Agropyron cristatum*
Grasses	Muttongrass	*Poa fendleriana*
Grasses	Tall wheatgrass	*Thinopyrum ponticum*
Grasses	Slender wheatgrass	*Elymus trachycaulus*
Grasses	Western wheatgrass	*Pascopyrum smithii*
Grasses	Cheatgrass	*Bromus tectorum*
Greasewood	Black greasewood	*Sarcobatus vermiculatus*
Shrubs	Big sagebrush	*Artemisia tridentata*
Shrubs	Shadscale saltbush	*Atriplex confertifolia*
Shrubs	Gray molly	*Bassia americana*
Shrubs	Broom snakeweed	*Gutierrezia sarothrae*
Trees	Utah juniper	*Juniperus osteosperma*

3.3 Estimation of Net Annual Primary Production

Net annual primary productivity has not been measured at the Clive site or in the adjacent vegetative associations. NAPP can vary widely on an annual basis and is strongly correlated with mean annual water availability, and in desert ecosystems, correlates moderately well with annual precipitation (Smith et al., 1997). Smith et al. (1997, Figure 7, p. 37) show Great Basin NAPP ranging from approximately 300 to 1500 kg/ha/yr, and report mean NAPP for Great Basin terrestrial systems of 920 kg/ha/yr. Given the lack of site-specific NAPP data, the variability of

NAPP, and the dependence of NAPP on annual water availability, it is reasonable to assume for the initial modeling effort that NAPP in the area of Clive has a uniform distribution of 300 to 1500 kg/ha/yr. A total biomass production for the selected plot is drawn from this distribution. Since these data are not on a per-plant or per-species basis, percent cover of each plant group will be used to apportion NAPP by vegetation type. This biomass is then apportioned based on the percent of vegetation from each plant type. Percent cover of each plant species was measured in 100 separate 1-m^2 quadrats located along ten transects in each Plot. Mean percent cover for each species was reported by SWCA (2011, Tables 1 through 5) for plant species recorded in each vegetation association, and this information is summarized by plant group in Table 4.

A distribution for percent plant cover was developed using a bootstrap resampling approach to estimate the sampling distribution of the mean percent plant cover (Efron 1998). The percent plant cover is to be applied for the full 10 ka performance period, and thus it is the distribution of the *mean* percent plant cover that is being modeled, to account for the time averaging. The bootstrap resampling simulation needs to reflect the same sort of sampling structure as the field sampling, in order to capture the underlying structure of the data. To simulate this structure, five transects from two subplots were selected at random from each plot, then 10 quadrats within those five transects were selected at random. This means that quadrat data originally within a transect were resampled together, and transect data from within a subplot were resampled together. Subplot data within a plot were resampled together, and data between plots were not mixed. As in standard bootstrap resampling, each random selection was done with replacement. A mean value was then calculated for percent cover of each plant type from the two subplots. To calculate total percent coverage, percent coverage for each plant type in each simulation was aggregated. The percent coverage for each plot, for each plant type, and for each simulation was saved in a table, with the entire process being repeated 1,000 times. Since data was collected on only two of the four subplots within a plot, there are only four ways in which the two subplots can be selected. Therefore, in this phase of the bootstrap resampling, all four possibilities are calculated and assigned equal weight. No standard statistical distribution provided an adequate fit to the resulting mean percent cover values. Thus, the simulated values were recorded in a table, and each simulated value is drawn with equal likelihood in the Clive PA GoldSim model. All percent cover simulation results are shown in the Clive PA Model Parameters Workbook.

To calculate total biomass by plant type, these percent cover simulations are used with the Total Biomass distribution to apportion biomass by plant type. For example, if a plot with 20% shrubs 30% grasses, and 50% bare ground is assumed to produce 1000 kg of biomass, 400 kg is assumed to be produced by shrubs and 600 kg is assumed to be produced by grasses (Table 5), since bare ground, which for purposes of this model includes litter and biological crust, is assumed to produce no biomass.

3.4 Root/Shoot Ratios

Distributions of above-ground and below-ground biomass production for plant groups will be developed from the total NAPP based on root/shoot ratio for each plant group. The root/shoot ratio is the ratio of below-ground (root) mass to above-ground (shoot) mass. Estimates of below-ground NAPP are determined by multiplying total NAPP by the root-shoot ratio of the species of concern. Above-ground NAPP is equivalent to the remaining portion of total NAPP. Root/shoot ratios for each plant group are shown in Table 6. A triangular distribution was developed for the

grasses root/shoot ratio. Data from Bethlenfalvay and Dakessian (1984, Table 2, p. 314) for *Hesperostipa comata* suggesting a root/shoot ratio of 1.2 in ungrazed systems was used for the mode of the distribution. Furthermore, since root/shoot ratios for grasses generally range from 1:1 to 2:1 (Neptune, 2005a) the endpoints of the distribution were set at a minimum of one and a maximum of two. For greasewood, the root/shoot ratio is based on information in Neptune (2005a) for creosote (*Larrea tridentata*), a warm desert shrub with a similar growth form to greasewood. The root/shoot ratio for the "Other Shrubs" category is based on the range of root/shoot ratios reported for sage (*Artemesia* spp) by Neptune, 2005a (Table 16, p. 38) . Utah juniper (*Juniperus osteosperma*) is the only tree found in any of the five survey plots. The root/shoot ratio for trees is based on western juniper (*Juniperus occidentalis*), a closely related species, as reported by Miller et al. (2005, p. 16). No root shoot information was available for the primary forbs occupying the site (halogeton and curveseed butterwort). This lack of information represents a data gap, though biointrusion modeling at NNSS showed that forbs, due to their more shallow rooting system and smaller contribution to NAPP, contributed very minimally to the biotic transport of buried wastes. To parameterize this model input, the root/shoot ratio for other shrubs was used, because this ratio represents a uniform distribution with a wide range and relatively large upper bound. For modeling of contaminant uptake, this means that the distribution tends to be conservative, since a large proportion of the plant mass can be determined to be underground, which results in increased absorption and upward movement of any contaminants in a given layer where roots occur.

Table 4. Measured percent cover of plant groups within each vegetation type (From Tables 1 through 5 in SWCA, 2011)

	Plot 1: Mixed Grassland	**Plot 2: Juniper - Sagebrush**	**Plot 3: Greasewood**	**Plot 4: Halogeton - Disturbed**	**Plot 5: Shadscale - Gray Molly**
% Tree	0	6.2	0	0	0
% Greasewood	0	0	4.5	0.2	0.2
% Other Shrub	2.0	18.9	0.6	5.0	13.1
% Forb	2.2	1.4	0.8	3.9	1
% Grass	26.4	9.8	0	0	0.1
% Bare Ground	69.4	63.7	94.1	90.9	85.6

Table 5. Great Basin net annual primary productivity

Group	Value or Distribution	Units	References
Total Biomass (Primary productivity)	U(300, 1500)	kg/ha/yr	Range for Great Basin from Smith, et al 1997. Mean of 920 kg/ha/yr reported by Le Houerou 1984. Net primary productivity dependent upon total moisture availability
Biomass Greasewood Biomass Shrubs Biomass Grasses Biomass Forbs Biomass Trees	Apportioned from above by % cover of each vegetation type		

Table 6. Root/shoot ratios for plant groups at Clive Site.

ES Plant Type	Value or Distribution	Units	References
Forbs	U(0.40, 1.80)	—	Distribution of “Other Shrubs” used for conservatism, see text
Grasses	Tri(1, 1.2, 2)	—	Based on *H. comata* (ungrazed), Bethlenfalvay and Dakessian, 1984
Greasewood	U(0.30, 1.24)	—	Assumed similar to creosote, from NTS (Neptune, 2005a)
Other Shrubs	U(0.4, 1.8)	—	Based on range for *Artemisia* spp. from Barbour, 1973
Trees	U(0.55, 0.76)	—	For Western Juniper, Miller et al, 2005

3.5 Maximum Root Depths and Biomass

Maximum root depths for each of the plant groups are based on literature values as shown in Table 7. Forbs are the most shallowly rooted plant group at Clive, with halogeton roots extending half a meter or less based on excavations conducted by SWCA (2011, Table 6). Though roots of some perennial grasses have been shown to extend up to two and a half meters (Zlatnik, 1999c), maximum rooting depths for the two most abundant grasses identified in the 2011 SWCA surveys of the Clive plots [needle and thread grass (*Hesperostipa comata*) and cheatgrass (*Bromus tectorum*)], extend about 1.5 meters (Zlatnik, 1999a, and Zouhar, 2003). Greasewood has been reported to extend taproots up to 19 meters to reach groundwater (SWCA Environmental Consultants, 2000, p. 2), though this extreme situation will only occur when precipitation can infiltrate to groundwater, as greasewood roots cannot penetrate the very dry soil that occurs below the zone of infiltration. The vegetative survey of the Clive site found that the majority of greasewood plants are less than one meter tall, and studies have found that greasewood of that size tend not to produce taproots (Robertson, 1983). Still, larger plants do occupy parts of the Clive site, especially where precipitation runoff is concentrated, and these plants may extend taproots to exploit deeper water. A maximum root depth of 5.7 meters (Robertson, 1983, p. 311) is used in this model. Maximum root depth for the "Other Shrub" category is based on rooting depths for shadscale as reported in Branson et al., (1976, Fig. 19, P. 1120). The maximum rooting depth of three shadscale excavated at the Clive site (Table 6 in SWCA, 2011) was approximately 75 cm. The proportion of root biomass as a function of depth was determined for greasewood, shadscale (i.e. other shrubs), and halogeton and mojave seablite (i.e. forbs) based on root profile excavations conducted by SWCA Environmental Consultants (2011) and is presented in Table 8. Maximum rooting depth for the only tree species found on any of the five survey plots (Utah juniper, *Juniperus osteosperma*) was based on rooting depths of the similar Western juniper (*Juniperus occidentalis*), which has been found to extend taproots as deep as 4.5 meters (Zlatnik, 1999b, p. 6). Understanding root biomass by depth is necessary to apportion below-ground biomass production to depth layers or "cells" within the cover component of the Clive PA model. The first step entails modeling the depth distribution of plant mass for each shrub and grass species. Once this is accomplished, a model is applied to the aggregate within each layer. The PA model utilizes the work done by Neptune (2005a) at NNSS to fit mathematical functions describing the root mass by depth for each of the plant groups. Fitting parameters (β) describing the root biomass as a function of depth for each of the Clive plant groups are presented in Table 9. All plant types use the same generic mathematical function to represent the density of roots with depth, from which is derived the value for f_i^N, the fraction of root in each layer *N*. Each plant type, however, is assigned specific distributions of parameter values z_i^{max} and β_i to change the shape of the function in order to fit available root density data.

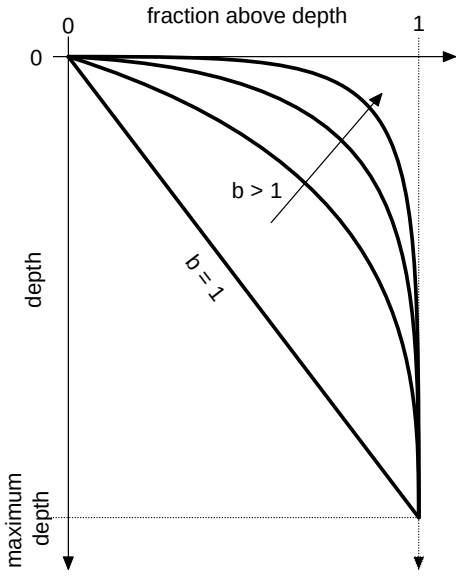

The function f_i used to represent root densities actually defines the fraction of all roots above any given depth. At depth $z = 0$, the value is obviously 0, and at the maximum

root depth $z = z_i^{max}$ the value is 1, meaning that all roots are above that depth (the definition of maximum root depth). The fraction of roots for plant *i* above any depth *z* is

$$f_i^z = 1 - \left(1 - \frac{z}{z_i^{max}}\right)^{\beta_i}. \quad \textbf{(1)}$$

Where:

f_i^z	Fraction of roots for plant *i* above any depth *z*
z_i^{max}	Maximum root depth for plant *i*
β_i	Fitting parameter for the root density equation, for plant *i*

A $\beta = 1$ indicates a uniform cylindrical "can-shape" distribution of roots from the surface to maximum rooting depth. Increasing β values result in a narrowing of overall rooting width with depth, with $\beta = 3$ resulting in a "cone-shaped" distribution of roots, and β values greater than 4 indicating increasingly "funnel-shaped" distributions with depth, as might be found in plants producing taproots. Neptune's work at the NNSS did not develop β parameters for forbs and trees. However, as shown in Table 8, excavations of halogeton, the dominant forb at the Clive site, show that all root mass is in the top 50 cm of soil. Tilley et al. (2008) report that halogeton does form a taproot that can extend to approximately 50 cm below the surface. Therefore, the selected β for forbs at Clive was based on the β for "other shrubs" at the NNSS, which though had deeper maximum rooting depths, had similar "shape" of root apportionment with depth. As discussed previously, the NNSS biointrusion modeling excluded evaluation of forbs due to their minimal contribution to the biotic transport of buried wastes. Additional excavations of halogeton to better define distribution of root mass with depth could be performed in the future if this uncertainty influences modeling results. Neptune's work at the NNSS also did not derive β parameters for trees. Therefore, the fitting parameter for juniper roots is based upon the β derived for creosote, which also forms a taproot and has a fairly deep maximum rooting depth [315 cm (Neptune, 2005a)] as that used here for juniper [450 cm (Zlatnik, 1999b)].

Table 7. Maximum root depths for plant groups at the Clive Site

ES Plant Type	Value or Distribution	Units	References
Forbs	51	cm	For Halogeton from Pavek, 1992
Grasses	150	cm	Based on *H. comata* (Zlatnik, 1999a) and *B. tectorum* (Zouhar, 2003), the two most abundant grasses at Clive
Greasewood	570	cm	Robertson, 1983
Other Shrubs	110	cm	Based on shadscale from Branson et al, 1976
Trees	450	cm	Value for Western Juniper from Zlatnik, 1999b

Table 8. Proportion root biomass by depth from Clive excavations conducted by SWCA Environmental Consultants (extrapolated by multiplying average number of roots per cm in each layer by the total rooting width in each layer, with all layers summing to 1)

Depth Interval (cm)	Proportion Rootmass in Layer					
	Black Greasewood		Other Shrubs		Forbs	
	Mean	St. Dev.	Mean	St. Dev.	Mean	St. Dev.
0-10	0.029	0.025	0.096	0.023	0.217	0.109
10-20	0.405	0.315	0.344	0.227	0.434	0.219
20-30	0.292	0.18	0.306	0.059	0.268	0.213
30-40	0.15	0.065	0.197	0.124	0.07	0.099
40-50	0.078	0.029	0.042	0.019	0.012	0.016
50-60	0.03	0.041	0.003	0.006	0	0
60-70	0.015	0.014	0.002	0.003	0	0
70-80	0.001	0.001	0.003	0.006	0	0
80-90	0	0	0.003	0.006	0	0
90-100	0	0	0.005	0.009	0	0

Table 9. Fitting parameter b describing root biomass above a given depth for each plant type

ES Plant Type	Value or Distribution	References
Forbs	N(μ=23.9 σ =0.313, min=1, max=Large)	Fitting parameter based on "other shrubs" at NNSS (Neptune, 2005a). See Section 3.5
Grasses	N(2.19, 0.036, min=1, max=Large)	Fitting parameter for perennial grasses (Neptune, 2005a)
Greasewood	N(μ=14.6, σ=0.0807, min=1, max=Large)	Based on fitting parameter for creosote at NNSS (Neptune, 2005a)
Other Shrubs	N(23.9, 0.313, min = 1, max=Large)	Based on fitting parameter for four-winged saltbush at NNSS (Neptune, 2005a)
Trees	N(μ=14.6 σ=0.0807, min=1, max=Large)	Based on fitting parameter for creosote at NNSS (Neptune 2005a). See Section 3.5

3.6 Estimation of Plant Uptake

Radionuclide concentrations in plant tissues are calculated based on root uptake using plant-soil concentration ratios ($K_{p\text{-}s}$), expressed as activity per dry weight plant tissue divided by activity per dry weight of bulk soil (Bq/g per Bq/g). Element-specific $K_{p\text{-}s}$ values were preferentially obtained from a recent publication of the International Atomic Energy Agency (IAEA, 2010). A report by Pacific Northwest National Laboratory (Staven et al., 2003) was used as a secondary reference when element-specific values were not available in IAEA (2010).

Element-specific values of $K_{p\text{-}s}$ were available in IAEA (2010) for all Clive PA radionuclides of concern with the exception of actinium, iodine, protactinium, and radon. For actinium and protactinium, americium values were employed as a surrogate as suggested in Staven et al., 2003). A $K_{p\text{-}s}$ value for iodine was obtained from Stave et al. (2003). A summary of $K_{p\text{-}s}$ values used in the Clive PA is provided in Table 10.

Distributional form for the values of geometric mean and geometric standard deviation reported in IAEA (2010) was not discussed in this reference. In order to provide a common set of inputs, values obtained from IAEA (2010) and Staven et al. (2003) were processed to conform to an assumed lognormal distribution. The value for iodine originally reported as an arithmetic mean was transformed to a geometric mean equivalent. $K_{p\text{-}s}$ data were reported in IAEA (2010) as a geometric mean, geometric standard deviation, minimum, and maximum. The geometric standard deviations are greater than 2 in nearly every case, suggested high right-skewness in the data, and the minimum and maximum were consistent with samples from a lognormal distribution. In order to establish a distribution for the mean, a parametric bootstrap approach was taken (Efron 1998), simulating bootstrap samples from the lognormal distribution using the maximum likelihood estimates of the lognormal parameters. A lognormal distribution was then fit to the resulting

bootstrap simulations of the mean, since some right-skewness was still present in the sampling distribution.

Plant-soil concentration ratios reflect an assumption that there is a linear and unchanging relationship between soil and plant tissue concentrations. In reality, $K_{p\text{-}s}$ values are liable to overestimate plant tissue concentrations as soil concentrations increase to levels higher than those employed in the studies from which the values are derived. This concern may apply in the Clive PA to conditions where plant roots are in contact with relatively high uranium concentrations, such as in disposed DU waste. The GoldSim model assumes that plant roots are in contact with soils in various layers belowground, each of which has its own concentration of contaminants ("Species" in GoldSim parlance). The roots present in each layer absorb each Species proportionally to the concentration of that Species in the soil in that layer. These absorbed Species are distributed uniformly throughout all the plant's tissues, aboveground and belowground. The plant is then assumed to die off, and all the Species contained within it are returned to soils in each layer according to the fraction of roots present in that layer. Aboveground plant parts are returned to the topmost soil layer. All of these processes take place in a single time step.

Table 10. Plant/soil concentration ratios

Element	Sample Size	Geometric Mean	Geometric St. Dev.	Notes
Actinium	27	0.0037	1.50	Americium used as a surrogate, based on Staven et al. (2003)
Americium	27	0.0037	1.50	
Cesium	401	0.67	1.13	
Iodine	1	0.066	3.87	Geo mean based on Staven et al. (2003). Geo SD from Sheppard and Evenden (1997).
Neptunium	16	0.095	1.35	
Protactinium	27	0.0037	1.50	Americium used as a surrogate, based on Staven et al. (2003).
Lead	34	0.29	1.54	
Plutonium	22	0.0010	1.35	
Radium	42	0.44	1.82	
Radon	NA	arbitrarily small number	1	Radon gas is inert and has effectively no potential to establish equilibrium in plant tissue.
Strontium	172	1.8	1.07	
Technetium	18	131	1.39	
Thorium	64	0.39	1.47	
Uranium	53	0.17	1.49	

The concentration of Species *j* in the plant *i* with roots in layer *N* is simply

$$C_{i,j}^{N} = CR_j \cdot C_s^N . \quad \textbf{(2)}$$

Where:

$C_{i,j}^{N}$ Concentration of Species *j* in plant *i* roots in layer *N*

CR_j Concentration ratio for all plants and Species *j* (Table 10)

C_s^N Concentration in soil on layer N

The total mass of Species *j* extracted by roots of plant *i* from soils (or wastes) in layer *N* is

$$M_{i,j}^{N} = C_{i,j}^{N} \cdot MP_i \cdot f_i^N \cdot f_{root} + C_{i,j}^{N} \cdot MP_i \cdot f_i^N \cdot f_{shoot} \quad \textbf{(3)}$$

Where:

f_i^{root} Mass fraction of plant *i* that is in the roots (belowground fraction)

f_i^N Mass fraction of root of plant *i* that is in layer *N* (so that the fraction of the entire plant in layer *N* is $f_i^{root} \times f_i^N$)

f_i^{shoot} Mass fraction of plant *i* that is in the shoots (aboveground fraction)

$M_{i,j}^{N}$ Mass of Species *j* extracted by the roots of plant *i* in layer *N*

MP_i Mass of all individuals of plant *i* over the site (M)

The model assumes that all absorbed Species are distributed uniformly throughout all the plant tissues, both aboveground parts and roots. The total mass of Species *j* in plant *i* is the total mass extracted by the roots of the plant summed across all *N* layers:

$$M_{i,j}^{T} = \sum_{N} M_{i,j}^{N} . \quad \textbf{(4)}$$

Where:

$M_{i,j}^{T}$ Total mass of Species *j* extracted by the roots of plant *i* and redistributed throughout the plant tissues

$M_{i,j}^{N}$ Mass of Species *j* extracted by the roots of plant *i* in layer *N*

This total amount of Species mass is divided up into the parts of the plant that occupy each layer, as well as the aboveground parts, so that we may calculate the mass of contamination ${}^{+}M_{i,j}^{N}$ that the plant returns to the various soil layers upon senescence. The total amount of contamination returned to the soils must equal the amount that was absorbed (not accounting for decay of the Species), in order to conserve mass of the Species. This total absorbed Species mass is returned to the soil in proportion to the amount of plant in each layer, with the topmost soil layer also receiving the aboveground plant parts:

$$\begin{aligned} {}^{+}M_{i,j}^{1} &= M_{i,j}^{T} \cdot f_{root} \cdot f_{i}^{1} + M_{i,j}^{T} \cdot f_{shoot} \\ {}^{+}M_{i,j}^{2} &= M_{i,j}^{T} \cdot f_{root} \cdot f_{i}^{2} \\ &\vdots \\ {}^{+}M_{i,j}^{N} &= M_{i,j}^{T} \cdot f_{root} \cdot f_{i}^{N} \end{aligned} \quad \textbf{(5)}$$

The net mass added to each layer is the redistributed mass from Equation 5 minus the absorbed mass from Equation 3. For plant *i*, this net mass added is simply

$${}^{+}M_{i,j}^{N} - M_{i,j}^{N}. \quad \textbf{(6)}$$

The GoldSim model contains various plant types. For the sake of simplicity in defining changes to each cell's inventory, the Species redistribution for all plants can be combined to result in a net addition (or subtraction) of mass effected by all plants. To do so, we sum Equation 6 over all the plant types:

$${}^{+}M_{j}^{N} = \sum_{i} {}^{+}M_{i,j}^{N} \quad \text{and} \quad M_{j}^{N} = \sum_{i} M_{i,j}^{N}. \quad \textbf{(7)}$$

4.0 Ant Specifications and Parameters

4.1 Ant Conceptual Model

Ants fill a broad ecological niche in arid ecosystems as predators, scavengers, trophobionts and granivores. However, it is their role as burrowers that is of main concern for the purposes of this model. Ants burrow for a variety of reasons but mostly for the procurement of shelter, the rearing of young and the storage of foodstuffs. How and where ant nests are constructed plays a role in quantifying the amount and rate of subsurface soil transport to the ground surface at the Clive site. Factors relating to the physical construction of the nests, including the size, shape, and depth of the nest, are key to quantifying excavation volumes. Factors limiting the abundance and distribution of ant nests such as the abundance and distribution of plant species, and intra-specific or inter-specific competitors, also can affect excavated soil volumes. Parameters related to ant burrowing activities include nest area, nest depth, rate of new nest additions, excavation volume, excavation rates, colony density, and colony lifespan. These attributes are described in this section, along with other considerations involving the impact of ant species and their inclusion in the Clive PA model.

The calculations of contaminant transport due to ant burrowing involves three steps:

1. Identify which of the ant species overwhelmingly contribute to the rearrangement of soils near the surface at Clive.

2. Calculate soil and contaminant excavated volume using maximum depth, nest area, nest volume, colony density, colony life span, and turnover rate for predominant ant species.

3. Calculate burrow density as a function of depth to determine the distribution of contaminants within the vertical soil profile for each predominant ant species.

4.2 Clive Field Surveys

Surveys for ants at Clive were limited to surface surveys of ant colonies, including identification of ant species, measurements (length, width, and height) of ant mounds, and determination of ant nest densities in each vegetative association (SWCA Environmental Consultants, 2011). No excavations of ant nests were performed at Clive to support the initial GoldSim model, though excavations could be conducted to support future model iterations if ant nest depth and volume are found to be sensitive parameters. Only two species of ants were identified during the surveys, with the western harvester ant, *Pogonomyrmex occidentalis*, accounting for 62 of the 64 nests identified. The second ant species, a member of the genus *Lasius*, was only encountered twice, both times in the mixed grassland plot. A summary of ant nests in each vegetative association is shown in Table 11.

Table 11. Summary of ant nests in each vegetative association

Vegetative Association	Number of Mounds/Hectare	Average Mound Surface Area (sq dm)
Plot 1: Mixed Grassland	33	95.03
Plot 2: Juniper-Sagebrush	2	39.77
Plot 3: Greasewood	7	120.18
Plot 4: Halogeton-disturbed	17	84.43
Plot 5: Shadscale-Gray Molly	6	137.73

4.3 Ant Nest Volume

Ant nests were not excavated at the Clive site, so only nest surface area – not nest volume or depth data was available. Generally, the surface areas of the Clive sites were smaller than the surface areas at the sites studied at the NNSS. To obtain estimates of nest volumes, a regression was made using *Pogonomyrmex* nest volume surface area data collected at the NNSS (Neptune, 2006) with nest surface area data described in Table 11. The NNSS data and associated regressions are shown in Figure 2. To be consistent with the data available from NNSS, the areas calculated are the two-dimensional areas of the mound – not the conical surface area.

To predict nest volume as a function of surface area, the following steps were taken:

1. Using data from NNSS, a linear model was fit to log transformed surface area and volume data to predict nest volume. Figure 2 shows the fitted model along with the predicted values based on measured surface area values from the Clive study.

2. To estimate the uncertainty in the predicted volume values, a model-based resampling method was used. With the statistical model created with the NNSS data, data from Clive were resampled with replacement. New values were estimated by drawing from a normal distribution whose mean was the predicted value and whose standard deviation is a function of both the fitting error and the residual error. This was repeated 10,000 times
3. The distribution of the mean volume is summarized by the mean and standard deviation of the resampled values.

Modeling all sample plots together resulted in a volume distribution of N(0.161m^3, 0.024 m^3). Predicted nest volumes were smaller than those observed at NNSS, where the volume distribution was N(0.64 m^3, 0.091 m^3).

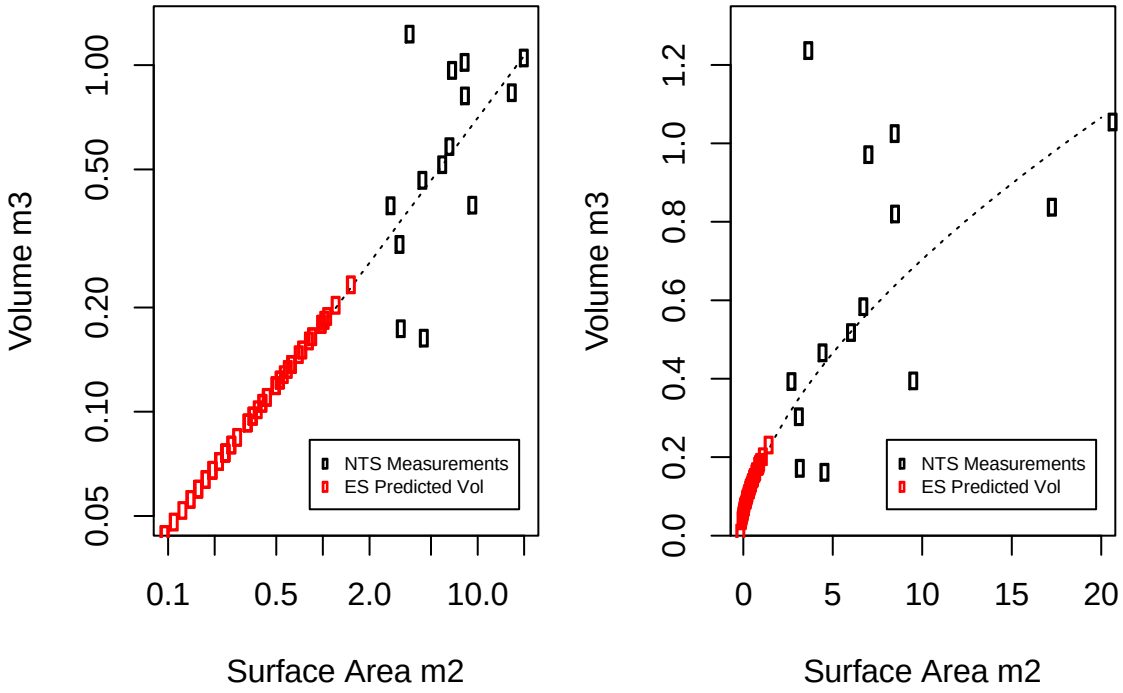

Figure 2. Linear regression model to predict ant nest volume based on nest surface area

4.4 Maximum Nest Depth

Again, since ant nests were not excavated, maximum nest depth had to be determined by other means. As shown in Figure 2, NNSS data support the assumption that larger mound surface area features correlate with larger nest volumes and deeper maximum depths, therefore the mound dimension data collected by SWCA (2011, Table 20, p. 23) was used to predict nest depths. The upper 95% prediction interval of SWCA-measured surface area was used with the NNSS linear model predicting depth as a function of surface area. The upper 95% prediction interval was used in lieu of a maximum value because taking the maximum of simulated values from an unbounded

normal distribution could result in an unrealistically large value. Using this approach, the predicted maximum nest depth at Clive is 212 cm.

4.5 Colony Lifespan

A critical component in modeling excavation volume is the turnover rate, or the fraction of the volume of the ant nest that is excavated in any given year. The turnover rate itself is inversely related to the life span of the colony. Table 12 shows four literature studies that report colony lifespan for *P. occidentalis* or *Pogonomyrmex* spp. These *Pogonomyrmex* spp. entries are included because the *P. occidentalis* study simply suggests colony lifespan is greater than 7 years, indicating that the study did not continue until colony failure. The non-specific studies include one entry that suggests a range of 15-20 yrs, one that suggests a range for the Queen of 17-30 but only 2-17 for the nest, and an entry of 20.2 ± 8.1 (standard deviation) based on 5 observations. The NNSS cover modeling (Neptune, 2006) used the latter entry, including the information that there were 5 data points. Since the standard deviation was based on 5 observations, the standard deviation of 8.1 was divided by the square of 5 to arrive at a normal distribution with a mean of 20.2 years and standard deviation of 3.6 years. This same distribution was used here. To ensure non-negative values as well as allow division by colony life, the distribution is truncated at 1e-20.

Table 12. Summary of *Pogonomyrmex* nest longevity reported in literature (Adapted from Neptune 2006, Table 6, p. 32)

Genera and species	Max nest (n) or queen (q) longevity (years)	Number of observations	Authors
Pogonomyrmex	17–30 (q)		Hölldobler and Wilson 1990
	2–17 (n)		Hölldobler and Wilson 1990
	20.2 ± 8.1	5	Porter and Jorgensen 1988
Pogonomyrmex occidentalis (Cresson)	>7 (n)		Hölldobler and Wilson 1990

4.6 Burrow Density as a Function of Depth

Excavation volume gives an overall picture of how much soil is being transported to the soil surface, however, it is also important to determine the density of burrowing activities as a function of depth within the vertical soil profile. The shape of the nest under the surface expression of the nest gives insight into the quantity of contaminated soils at various depths being excavated to the surface. The burrow density as a function of depth is described by the fitting

parameter β. Lacking site-specific nest excavations at Clive, the fitting parameter developed in the NNSS study (Neptune, 2006) for all *Pogonomyrmex* species is used in the model. Based on bootstrapping, a normal distribution with a mean of 10 and standard deviation of 0.71, truncated at 1, was estimated for β (Figure 4) for *Pogonomyrmex* nests at NNSS (Neptune, 2006).

4.7 Colony Density

Colony densities in the five Clive plots ranged from two colonies per hectare in the Juniper-Sage habitat to 33 colonies per hectare in the mixed grassland (SWCA 2011, Table 20, p. 23). For the initial model, the colony density will use the non-informative prior distribution and the Bayesian posterior, meaning that for an observed count of X, the posterior distribution for the rate would be Gamma(X, 1) (where the 1 is in the units of data collection, i.e. 1/ha). Expressed another way, Bayesian statistics combines knowledge about a process generating data (in this case colony counts) with assumptions about the process. It is reasonable to assume that the colony counts are non-negative - making the gamma distribution more appropriate than a normal distribution. A non-informative prior indicates that other than the fact that counts cannot be negative, there is no data which might suggest how the colony counts are distributed for each location. In other circumstances, other data might be used to reduce uncertainty. In this case, the distributions are conservative and reflect this lack of prior knowledge. Figure 3 illustrates the shape of the distributions used to describe colony counts for each plot area.

Modeling soil and contaminant transport by ant species within the Clive PA model assumes that ants move materials from lower cells to those cells above while excavating chambers and tunnels within a nest. These chambers and tunnels are assumed to collapse over time and return soil from upper cells back to lower cells. Through this process the balance of materials is preserved through time. Soil and contaminant movement from one cell to another is calculated as follows. Within each layer, the fraction of excavated ant nest volume and the fraction of contaminants contained within that layer are determined. The fraction of contaminants within the excavated volume is based on the ratio of the excavated volume to total volume of each layer and is assumed to be distributed homogeneously within the layer. Secondly, the sum of contaminants from each layer associated with ant nest is calculated with the assumption that all excavations from layers below are deposited in the uppermost layer. Finally, downward movement of contaminants associated with chamber and tunnel collapse from each layer to the layer below is calculated and the net movement of contaminants into each layer is determined. The amount of contaminants in each layer is then used to adjust contaminant inventory in each layer for the next time step.

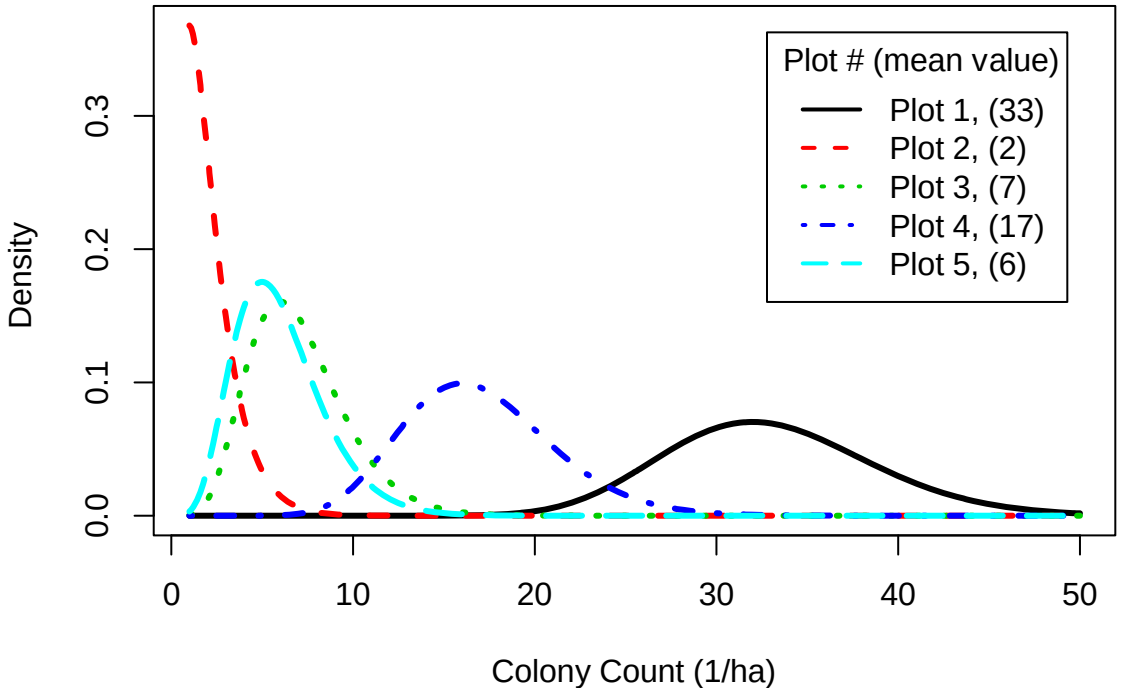

Figure 3 Distribution of ant colony counts for each plot area.

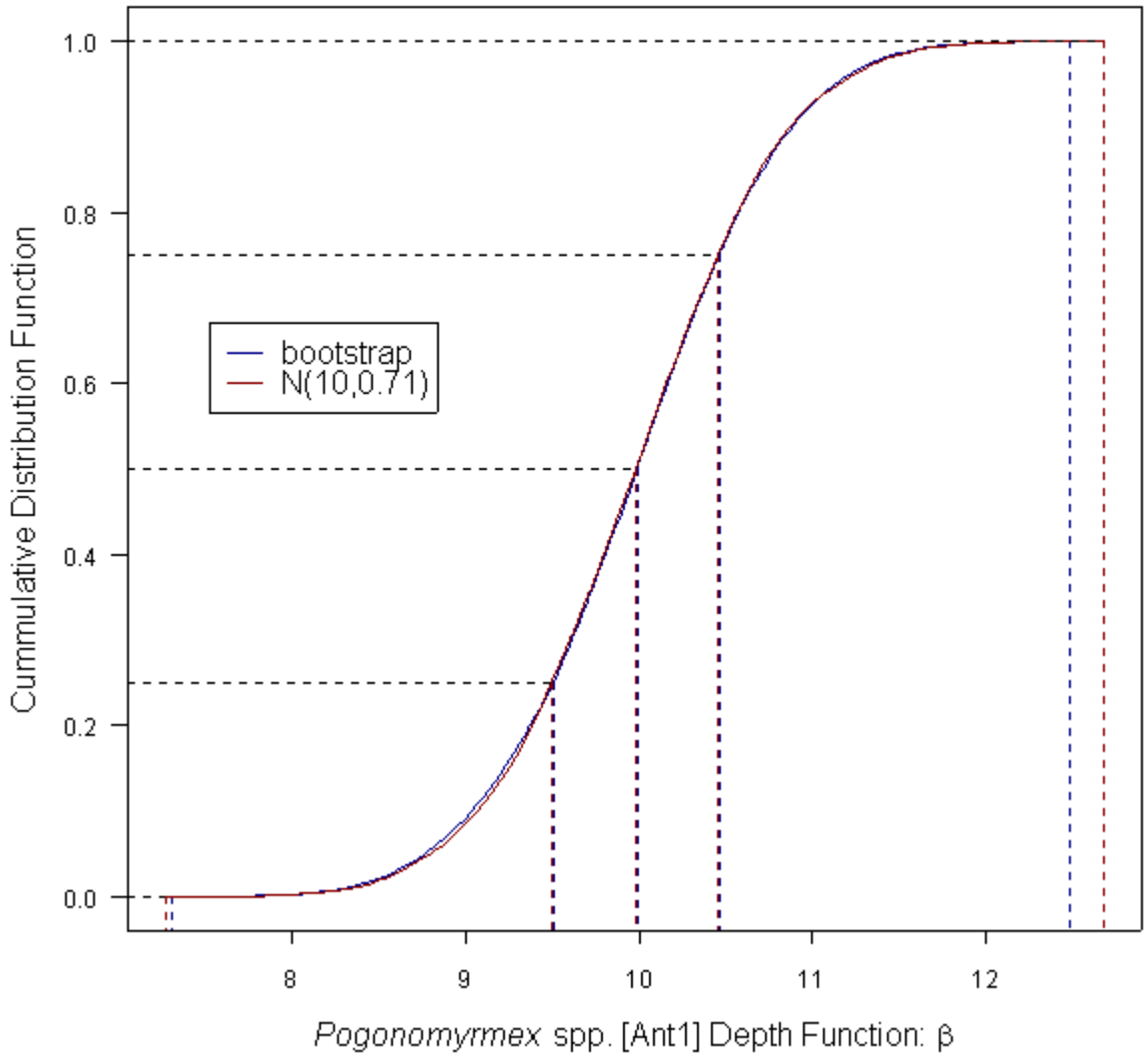

Figure 4. Comparison of bootstrapped and a normal distribution for *Pogonomyrmex spp.* nest density with depth β parameter

5.0 Mammal Specifications and Parameters

5.1 Mammal Conceptual Model

Burrowing mammals can have a profound impact on the distribution of soil and its contents near the soil surface. The degree to which mammals influence soil structure is dependent on the behavioral habits of individual species. While some species account for a large volume of soil displacement, others are less influential. This section presents the functional factors used to parameterize the Clive PA model. Factors such as burrowing depth, burrow depth distributions, percent burrow by depth, tunnel cross-section dimension, tunnel lengths, soil displacement by weight, soil displacement by volume and animal density per hectare play a critical role in determining the final soil constituent mass by depth within the soil.

Modeling soil and contaminant transport by mammal species within the Clive PA model assumes animals move materials from lower cells to those cells above while excavating burrows. Furthermore, burrows are assumed to collapse over time and return soil from upper cells back to lower cells (Figure 5). Thus, the balance of materials is preserved through time. Calculating soil and contaminant movement from one cell to another is straightforward. Within each layer, the fraction of burrow volume and the fraction of contaminants contained within the burrowed volume are determined. The fraction of contaminants within the burrowed volume is based on the ratio of burrow volume to total volume of each layer and is assumed to be distributed homogeneously within the layer. Secondly, the sum of contaminants from each layer associated with burrow excavation by all animal types is calculated with the assumption that all excavations from layers below are deposited in the uppermost layer. Finally, downward movement of contaminants associated with burrow collapse from each layer to the layer below is calculated and the net movement of contaminants into each layer is determined. The amount of contaminants in each layer is then used to adjust contaminant inventory in each layer for the next time step.

The calculations of contaminant transport due to mammal burrowing involves four steps:

1. Identify which of the mammal species overwhelmingly contribute to the rearrangement of soils near the surface.

2. Assign these mammal species to categories and determine the excavated volumes.

3. Calculate burrow density as a function of depth for mammal categories.

4. Determine the distribution of the burrow depth fitting parameter β for mammal categories.

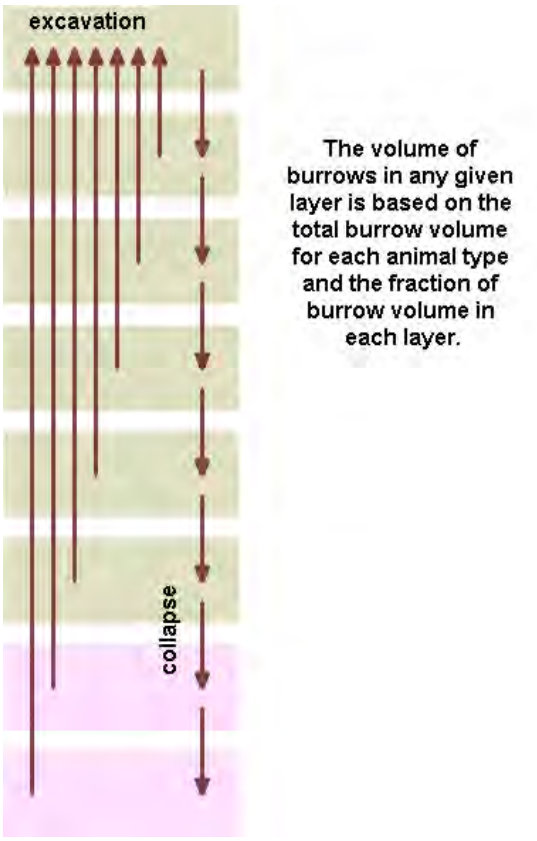

Figure 5. Conceptual diagram of soil movement by burrowing animals

5.2 Clive Site Surveys

Each Clive plot was surveyed for small mammal burrows during September and October 2010 (SWCA 2011). Burrows were identified by animal category, as shown in Table 13. Within the survey area four categories of mammal burrows were identified: ground squirrels, kangaroo rats, mouse/rats/voles, and one badger. Due to the small number of badger and ground squirrel burrows, the decision was made to treat all burrowing mammals as a single unit for modeling purposes. Small mammal trapping was conducted on the five Clive plots during the new moon in October 2010 to identify the principal small mammal fauna present in each vegetative association. Each 1.0-ha plot was subdivided into 25 20–m × 20–m subplots. At the center of the each subplot, two Sherman® live traps were placed, for a total of 50 traps per plot. Results of the small mammal trapping are presented in Table 14.

Table 13. Summary of Clive small mammal burrow surveys

	Badger	Ground Squirrel	Kangaroo Rat	Mouse/Vole/ Rat	Total
Plot 1: Mixed Grassland	0	2	102	131	235
Plot 2: Juniper-Sage	1	0	222	16	239
Plot 3: Greasewood	0	1	1	1	3
Plot 4: Halogeton-disturbed	0	0	0	0	0

Plot 5: Shadscale-Gray Molly	0	0	0	1	1

Deer mice (*Peromyscus maniculatus*) were the most abundant small mammal captured during trapping, and were the only mammal captured in the plots located on the Clive facility (Plots 3, 4, and 5). Plots 3, 4, and 5 were characterized by very low mammal densities, as evidenced by both the trapping results and the burrow surveys. With such a small population in plots 3, 4, and 5, the decision was made to average these plots. Similar to how the ant mound density data was used to develop distributions for the model, the resulting mammal burrow population counts were used to develop Gamma distributions for mound density. For the GoldSim model mound density is defined as Gamma(X, 1) where X is the number of mammal mound counts for each plot.

5.3 Mound Volume

After burrow surveys were completed, soil volumes were collected in a randomly selected ¼-plot (0.25 ha) within each plot. The obviously mounded or disturbed soil around a burrow entrance was collected and its volume measured. This provides an estimate of the volume of soil excavated to the surface from each burrow, with the assumption that the mounded soil represents excavations for a single year. Results of the mound volume measurements are shown in Table 15. Based on analysis of the data presented in Table 15, the per-mound volume is defined as a normal distribution with a mean of 0.0006 m^3/yr, and a standard deviation of 0.00015 m^3/yr. Total annual excavated volume is equal to the per mound volume multiplied by the mound density.

5.4 Maximum Burrow Depth

Maximum burrow depth was set at 200 cm based on best professional judgment. This depth is consistent with that used at NNSS by Neptune (2005b), and represents the likely average vertical extent of multiple badger excavations (Kennedy et. al, 1985).

5.5 Burrow Density as a Function of Depth

The β parameter describes the burrow density as a function of depth, and alters the form and volume of the excavated burrow. As the value of β increases, the fraction of burrow excavated at each depth moves from being evenly distributed to a highly skewed distribution with most of the excavation occurring near the soil surface. Since no below-ground measurements were obtained on mammal burrows at Clive, this version of the PA model uses the β parameter derived by Neptune (2005b) for rodents at NNSS. The β parameter, defined based on analysis of NNSS data, resulted in a parameter estimate of 4.5 and a standard error of 0.84. Badger data were not used in the derivation of the β parameter do to the overall scarcity of badgers in the survey area, where only one badger burrow was recorded in the five hectares surveyed across all vegetation types.

Table 14. Results of Clive small mammal trapping

Plot	Date	Species	Count - Species	Sum - # Recaptured	Sum - # Deceased
1			24	7	3
	10/5/2010		4	0	0
		Peromyscus maniculatus	4	0	0
	10/6/2010		4	0	1
		Peromyscus maniculatus	4	0	1
	10/7/2010		8	3	1
		Peromyscus maniculatus	6	3	1
		Dipodomys microps	1	0	0
		Onychomys leucogaster	1	0	0
	10/8/2010		8	4	1
		Peromyscus maniculatus	8	4	1
2			43	5	0
	10/5/2010		7	0	0
		Peromyscus maniculatus	7	0	0
	10/6/2010		8	2	0
		Peromyscus maniculatus	8	2	0
	10/7/2010		14	0	0
		Peromyscus maniculatus	10	0	0
		Dipodomys microps	3	0	0
		Dipodomys ordii	1	0	0
	10/8/2010		14	3	0
		Peromyscus maniculatus	11	3	0
		Dipodomys microps	3	0	0
3			2	1	0
	10/6/2010		1	0	0
		Peromyscus maniculatus	1	0	0
	10/7/2010		1	1	0
		Peromyscus maniculatus	1	1	0
4			1	0	0
	10/8/2010		1	0	0
		Peromyscus maniculatus	1	0	0
5			4	1	0
	10/6/2010		1	0	0
		Peromyscus maniculatus	1	0	0
	10/7/2010		1	0	0
		Peromyscus maniculatus	1	0	0
	10/8/2010		2	1	0
		Peromyscus maniculatus	2	1	0
Total			74	14	3

Table 15. Soil volume (m^3) of excavated mammal burrows

Plot	Burrow ID	Number of Burrows	Kangaroo Rat	Mouse/Vole/Rat	Badger	Grand Total
1			0.01203	0.00059		0.01262
	1SW104	2	0.0035			0.0035
	1SW105	1		0.00001		0.00001
	1SW106	2		0.0002		0.0002
	1SW107	1		0.00001		0.00001
	1SW108	1	0.00005			0.00005
	1SW110	1	0.00125			0.00125
	1SW111	2	0.0003			0.0003
	1SW112	4	0.00056			0.0006
	1SW113	1		0.00003		0.00003
	1SW114	1		0.00001		0.00001
	1SW115	1	0.00025			0.00025
	1SW116	1	0.00005			0.00005
	1SW117	3	0.0025			0.0025
	1SW118	4		0.00008		0.00008
	1SW119	1	0.00003			0.00003
	1SW120	1	0.00003			0.00003
	1SW121	3	0.00009			0.00009
	1SW122	2	0.00003			0.00003
	1SW123	1	0.00003			0.00003
	1SW124	1	0.0002			0.0002
	1SW125	1	0.00015			0.00015
	1SW126	1	0.0001			0.0001
	1SW127	1		0.00001		0.00001
	1SW128	4	0.00286			0.00286
	1SW129	1	0.00005			0.00005
	1SW130	1		0.00004		0.00004
	1SW131	2		0.00005		0.00005
	1SW132	2		0.00003		0.00003
	1SW133	1		0.0001		0.0001
	1SW134	1		0.00002		0.00002
2			0.037845	0.00019	0.006	0.044035
	2NE002	1	0.00005			0.00005
	2NE006	1		0.00001		0.00001
	2NE007	1	0.00001			0.00001
	2NE009	6	0.00015			0.00015
	2NE010	1		0.06000		0.00006
	2NE012	1	0.000225			0.000225
	2NE015	1			0.006	0.006
	2NE019	2	0.00135			0.00135

Plot	Burrow ID	Number of Burrows	Kangaroo Rat	Mouse/Vole/Rat	Badger	Grand Total
	2NE020	11	0.00683			0.00683
	2NE021	14	0.002975			0.002975
	2NE025	1	0.00006			0.00006
	2NE026	3	0.000185			0.000185
	2NE027	1		0.0001		0.0001
	2NE028	1	0.00005			0.00005
	2NE029	1	0.0002			0.0002
	2NE037	1		0.00001		0.00001
	2NE040	1	0.00001			0.00001
	2NE041	4	0.00004			0.00004
	2NE044	1		0.00001		0.00001
	2NE046	3	0.0003			0.0003
	2NE048	2	0.0001			0.0001
	2NE051	10	0.01501			0.01501
	2NE052	3	0.0095			0.0095
	2NE104	2	0.0008			0.0008
3				0.001		0.001
	3NE003	1		0.001		0.001
5				0.01375		0.01375
	5SW001	1		0.01375		0.01375
Grand Total		124	0.049875	0.01553	0.006	0.071405

6.0 References

Bethlenfalvay, G.J., and S. Dakessian. 1985. Grazing effects on mycorrhizal colonization and floristic composition of the vegetation on a semiarid range in Northern Nevada. *J. Range Management*. 37(4): 312-316.

Branson, F.A., Miller, R.F., and I.S. McQueen. 1976. Moisture relationships in twelve northern desert shrub communities near Grand Junction, Colorado. *Ecology*. 57: 1104-1124.

Efron B., and Tibshirani R.J. 1998. Introduction to the Bootstrap, CRC Press, Boca Raton, FL.

Hölldobler B. and E.O. Wilson. 1990. The Ants. The Belknap Press of Harvard University Press, Cambridge, Massachusetts. 732 pp.

IAEA, 2010. *Handbook of Values for the Prediction of Radionuclide Transfer in Terrestrial and Freshwater Environments*, Technical Report Series No. 472, International Atomic Energy Agency, Vienna, 2010.

Kennedy, W.F., L.L. Cadwell, and D.H. McKenzie. 1985. Biotic transport of radionuclide wastes from a low-level radioactive waste site. *Health Physics* 49(1): 11–24.

Neptune. 2005a. Plant Parameter Specifications for the Area 5 and Area 3 RWMS Models. Neptune and Company, Inc.

Neptune. 2005b. Mammal Parameter Specifications for the Area 5 and Area 3 RWMS Models. Neptune and Company, Inc.

Neptune. 2006. Ant Parameter Specifications for the Area 5 and Area 3 RWMS Models. Neptune and Company, Inc.

Pavek, Diane S. 1992. *Halogeton glomeratus*. In: Fire Effects Information System, [Online]. U.S. Department of Agriculture, Forest Service, Rocky Mountain Research Station, Fire Sciences Laboratory (Producer). Available: http://www.fs.fed.us/database/feis/ [2011, February 22]

Robertson, J.H., 1983. Greasewood (Sarcobatus vermiculatus (Hook.) Torr.). *Phytologia*. 54(5): 309-324.

Sheppard, S.C. and W.G. Evenden. 1997. Variation in Transfer Factors for Stochastic Models: Soil-to-Plant Transfer, *Health Physics*, 72: 727-33.

Smith, S.D., Monson, R.K., and J.E. Anderson. 1997. *Physiological Ecology of North American Desert Plants*. Springer-Verlag, Berlin. 286 pages.

Staven L.H., Napier B.A., Rhoads K., Strenge DL. 2003. *A Compendium of Transfer Factors for Agricultural and Animal Products,* Pacific Northwest National Laboratory, Richland WA.

SWCA Environmental Consultants. 2000. *Assessment of Vegetative Impacts on LLRW*. Prepared for Envirocare of Utah, Inc. Salt Lake City, UT. 12 pages.

SWCA Environmental Consultants. 2011. *Field Sampling of Biotic Turbation of Soils at the Clive Site, Tooele County, Utah*. Prepared for Energy Solutions, Salt Lake City, UT. 31 pp.

Tilley, D., Ogle, D., and L. St. John. 2008. Halogeton, *Halogeton glomeratus* (M. Bieb.) C. Meyer. USDA NRCS Plant Guide. United States Department of Agriculture. Available: http://plants.usda.gov/plantguide/pdf/pg_hagl.pdf [2011, May 11]

Zlatnik, Elena. 1999a. *Hesperostipa comata*. In: Fire Effects Information System, [Online]. U.S. Department of Agriculture, Forest Service, Rocky Mountain Research Station, Fire Sciences Laboratory (Producer). Available: http://www.fs.fed.us/database/feis/ [2011, February 22].

Zlatnik, Elena. 1999b. *Juniperus osteosperma*. In: Fire Effects Information System, [Online]. U.S. Department of Agriculture, Forest Service, Rocky Mountain Research Station, Fire Sciences Laboratory (Producer). Available: http://www.fs.fed.us/database/feis/ [2011, February 22].

Zlatnik, Elena. 1999c. *Agropyron cristatum*. In: Fire Effects Information System, [Online]. U.S. Department of Agriculture, Forest Service, Rocky Mountain Research Station, Fire Sciences Laboratory (Producer). Available: http://www.fs.fed.us/database/feis/ [2011, February 22].

Zouhar, Kris. 2003. *Bromus tectorum*. In: Fire Effects Information System, [Online]. U.S. Department of Agriculture, Forest Service, Rocky Mountain Research Station, Fire Sciences Laboratory (Producer). Available: http://www.fs.fed.us/database/feis/ [2011, February 22].